

Preparation, Characterisation and Physicochemical Properties of Cellulose Nanocrystals from Cassava Peel

C. V. Abiaziem^{1,2*}, A. B. Williams¹, A. I. Inegbenebor¹, C. T. Onwordi,^{3,4} , L. F. Petrik³

¹Department of Chemistry, Covenant University, Km 10, Canaan Land, Ota, P.M.B 1023, Ota, Ogun State, Nigeria

²Science Laboratory Technology Department, The Federal Polytechnic Ilaro, P.M.B 50, Ilaro, Ogun State, Nigeria

³Department of Chemistry, Environmental and Nano Sciences Group, University of the Western Cape, Bellville, Cape Town, 7535, South Africa

⁴Department of Chemistry, Lagos State University, Ojo, LASU P.O.Box 0001, Ojo, Lagos State, Nigeria

*Corresponding author: vyvycox@yahoo.com

Abstract.

This study was carried out to investigate the potential use of cassava peel as a source of cellulose and nanocrystalline cellulose. Isolation of cellulose from cassava peel was prepared by using two pretreatments methods; alkaline treatment and bleaching with acidified sodium chlorite. Acid hydrolysis was performed at 45°C for 45 mins using 64% concentration sulphuric acid. The extracted cellulose nanocrystal (CNC) of the cassava peel was characterised using, scanning electron microscope (SEM), x-ray diffraction (XRD), transmission electron microscopy (TEM), fourier transformed infrared spectroscopy (FTIR), thermogravimetric analysis (TGA) and zeta potential analysis. Physicochemical properties of the samples were studied. From the SEM images, features of the cellulose nanocrystal in the cassava peel, showed that there was a reduction in the fibrillar structure size and intermittent breakdown in fibrillar structure into individualize fibrils; the TEM images showed that the cassava peel sample is spherical in shape, conglutinated and fixed with each other. The FTIR spectra of the CNC was identified as cellulose structures that showed effective removal of amorphous materials. XRD showed that the crystallinity index increased progressively from the raw to the CNC with CNC crystallinity index of 99.86 % and a particle size of 5.56 nm. The TGA curve revealed a good thermal stability for CNC. The Zeta Potential revealed a negative surface charge of -20.7 ± 8.12 mV and a polydispersity index of 0.633. The results showed effective extraction of CNC from cassava peel (a waste material from agricultural process). This material has potential for various industrial applications such as in medicine, adsorption of toxic metals, bio-nanocomposites, food packaging etc.

Keywords: Cassava peel, cellulose nanocrystals, acid hydrolysis, characterization, agricultural waste

1.0 Introduction

There is a growing concern towards the useful utilization of agro-industrial waste, such as, cassava bagasse and peel, sugarcane bagasse and peel as raw materials for various industrial applications (Widiarto et al., 2017; Wulandari et al., 2016). Cassava is the fifth most abundant starch crop produce in the world and one of the most important food sources. The peels of cassava is rarely used and it is a cellulosic material (Widiarto et al., 2017).

The increasing development of nanotechnology, and fast depletion of petroleum resources have prompted the quest for a new environmentally friendly materials gotten from natural resources, comprising of cellulose (Pelissari et al., 2013; Julie et al., 2016). Cellulose, is one of the most early and abundant natural polymer on earth which draws more attraction in a new form called nanocellulose (Julie et al., 2016). The production of nanocellulose fibres has gained increasing attention due to their high strength, stiffness, availability, biocompatibility, large surface to volume ratio, high tensile strength, flexibility as well as excellent diverse mechanical, electrical, sustainability and thermal properties (Rumpoko et al., 2013; Pelissari et al., 2013). Cellulose constitutes of β -1, 4-linked anhydro-D-glucose units and have hydroxyl (-OH) groups that makes it to build bonds of hydrogen which are strong and they are hydrophilic polymers. The origin of cellulose are; banana rachis, sugarcane bagasse, soy hulls, corncob, cassava bagasse, wood, hemp, mengkuang leaves (*Pandanus tectorius*), rice husk, kapok fruit, jute, sweet potatoes residue, capim dourado etc. (Anuj et al., 2014; Moran et al., 2008). In overall, plant cell walls consist mainly of three organic compounds, which include cellulose, hemicellulose, and lignin. Natural lignocellulosic materials are the primary components of these organic compounds (Chen, 2014; Yang, 2008). Due to the size and morphology, nanocellulose fibre is congregated as cellulose nanocrystals (CNC), cellulose nanowhiskers, cellulose nanofibers and bacterial cellulose or microbial cellulose (Julie et al., 201; Dufresne, 2012). These cellulose nanofibers have gained much attention from researchers, due to their applications in various areas: in the biomedical field, as reinforcement agents in nanocomposites, food packaging, as fuel cell membranes etc (Pelissari et al., 2013). Cellulose nanofibres are discovered as green reinforcement alternatives to synthetic fibers for varied applications. Natural cellulosic fibers have several merits over conventional materials such as extensive toughness, flexibility, recyclability, and eco-friendliness (Leite et al., 2016).

The method used to extract and isolate cellulose, especially as nanofibres, must be modified for each parent material. The isolation procedure involves structural breakdowns through pretreatments, usually alkaline hydrolysis, followed by acid hydrolysis, to afford isolated nanofibres with high crystallinity and to reduce the amount of amorphous material (Leite et al., 2016; Abdul et al., 2012). Both hemicellulose and lignin are amorphous polymers. Amorphous region and isolation of nanocellulose crystals from natural fibers are removed by a well-known strong acid hydrolysis process. Under monitored conditions, acid hydrolysis allows removal of the amorphous regions of cellulose fibres while the crystalline regions are intact in the form of crystalline nanocrystals. Moreover, removal of the amorphous region impacts the structure, thermal stability, crystallinity as well as surface morphology of the fibres (Ilyas et al., 2018, Ilyas et al., 2017). However, different methods have been used to achieve highly purified nanocrystals from cellulosic materials. These methods include chemical method, which was majorly performed by acid hydrolysis, mechanical treatments, grinding and ultrasonication (Hongjia et al., 2013; Elazzouzi-hafraoui et al., 2008, Li et al., 2009; Abe and Yano, 2010; Wang and Cheng, 2009). All of the above methods can be used to prepare different types of nanocrystal materials, depending on the cellulose parent material and its pretreatment. Sulphuric acid hydrolysis is a common

method which is used to prepare cellulose nanofibers, due to its ability to disintegrate amorphous domains, it also presents negative charges to the surface nanoparticles (Hongjia et al., 2013; Beck-Candanedo et al., 2005), and produce stable nanocrystal suspensions. The Ultrasonic technique has been used to isolate cellulose nanocrystals in current years. The ultrasonic method also gradually disintegrates the micron-sized cellulose fibers into nanocrystals.

The goal of this present work was to extract cellulose nanocrystals from cassava peel using sodium hydroxide treatment, sodium chlorite as bleaching agent for the removal of lignin and under different conditions of sulphuric acid hydrolysis for the complete removal of amorphous region while the crystalline region is intact and characterize it in order to achieve a material with a high crystallinity index, high thermal stability and morphology suitable for various applications such as a reinforcement agent in the production of nanocomposites, adsorbent for water treatment, food packaging etc. The choice of cassava peel to produce cellulose nanocrystal is because of its availability as an agro industrial waste which is in large quantity in Ogun state, Nigeria.

In this study, several techniques were employed to characterize the raw cassava peel, the treated cassava peel (cellulose) and the cellulose nanocrystals from cassava peel. It was characterized by fourier transform infrared spectroscopy (FTIR), x-ray diffraction (XRD), thermogravimetric analysis (TGA), zeta potential. The morphological features of the cellulose and nanostructures were evaluated by scanning and transmission electron microscopy (SEM and TEM) and various physicochemical parameters were carried out on the cassava peel, to investigate the potential use of cellulose nanocrystals isolated from the cassava peel as a prospect for various industrial applications.

2.0 Experimental

2.1 Materials and Methods

Cassava peel used in this study was collected from different cassava processing factory at Ilaro area in Ogun State, Nigeria. Sodium hydroxide pellets (98%), Sulfuric acid (95-99%), Toluene (99%) and Sodium chlorite (23-26%) were purchased from Merck chemicals South Africa. Cellulose dialysis membranes of 12–14 kDa molecular weight cut off (Sigma-Aldrich, South Africa) were purchased from Sigma Aldrich. Ethanol (99%) and Acetic acid (99.8%) were purchased from Kimix Chemicals, South Africa. Reagents and chemicals were used as a laboratory grade without purification. All water used was ultra-pure water (Millipore Milli-Q UF Plus).

2.2. Isolation of Cellulose Fibre from Cassava Peel

Chemically purified cellulose (CPC) from cassava peels were isolated according to the previously reported methods with minor modifications by Lu and Hsieh, 2012, Rahimi et al., 2016, Shaheen and Emam, 2018, Anuj et al., 2014, Abe et al., 2007; Abe and Yano, 2009. The peels of cassava were prepared by washing with warm water, followed by sun drying. The clean dried sample was milled and allowed to pass through a 30 mesh screen. The cassava peel (30 g) was extracted with 2:1 v/v toluene and ethanol mixture for 6 h to remove wax, oil and pigments and then allowed to dry in an oven at 60°C for 16 h. The dewaxed fibres were successively treated with 300 ml water at 55 °C, to remove water-soluble components with the residue being filtered and washed until neutral pH. The samples were then dried in an oven at 60 °C for 16h. The dewaxed samples were soaked in 50 g/L of 5% sodium hydroxide solution at

25 °C for 24 h and at 90 °C for 2 h to remove hemicellulose and silica. This was washed with copious amount of distilled water until the filtrate became neutral, followed by drying at 50 °C for 16 h. The residual alkaline treated samples were then delignified using 2.5 % w/v of acidified sodium chlorite with pH adjusted to 4 with acetic acid using material to liquor ratio 1:20 for 4 h at 100 °C. The delignified cellulose was finally washed with water to remove the excess/unreacted chemicals and dried in the oven at 50 °C for 16 h. Finally, the product (chemically purified cellulose CPC) was stored in air tight container.

2.3 Synthesis of Cellulose Nanocrystals

Chemically purified cellulose (α -cellulose) produced from peels of cassava was synthesized to cellulose nanocrystals by acid-hydrolysis, according to the method adopted by (Ilyas et al., 2018, Naduparambath et al., 2018; Rahimi et al., 2016; Anuj et al., 2013 and Lu and Hseih, 2012) with little modifications. The cellulose isolated from cassava peel was hydrolysed with 64 wt% sulphuric acid at a 10 mL/g acid-to-cellulose ratio at a temperature of 45 °C for 45 minutes with vigorous mechanical stirring. Reaction of hydrolysis was stopped by diluting with 10-fold ice water. The resultant cellulose nanocrystal gel was centrifuged at 45000 rpm for 30 minutes to concentrate the cellulose nanocrystals and to remove excess aqueous acid, the filtrate was then decanted. The resultant precipitate was dialyzed with cellulose dialysis membranes of 12–14 kDa molecular weight cut off (Sigma-Aldrich, South Africa) against ultra-pure water (Millipore Milli-Q UF Plus) until reaching neutral pH (pH 6-7). The suspension was sonicated at an amplitude of 40% in an ice bath to disrupt solid aggregates and avoid overheating. The resultant CNC suspension was freeze-dried (–47 °C, 0.2mbar). The dried sample was stored in an air tight container for characterization.

2.4 Characterisation

2.4.1 Chemical Composition

The chemical compositions of cassava peel was determined according to the method by Ayeni et al., 2015. The raw fibre, alkali-treated fibre and the bleached fibre were measured at different stages of treatment. The percentage extractives (wax), percentage hollocellulose, percentage lignin and percentage cellulose were determined.

2.4.2 Yield of CNC

The percentage yield of the cassava peel was calculated as percentage of initial weight of cassava peel cellulose (CPC) after treatment with sulphuric acid. The weight of the freeze-dried sample after acid hydrolysis was compared with the initial weight of RSP. Weight of samples final of CPCNCs, M_f and initial of CSP, M_i were determined in order to calculate the yield (Ilyas et al., 2018, Bondeson et al., 2006a). Yield was calculated by using Equ. (1).

$$\text{Yield} = M_f/M_i * 100 \dots \dots \dots \text{Equ. 1}$$

2.4.3 FTIR was used to determine the functional groups of a molecule. The technique evaluates the physical differences on samples due to treatments by chemicals. In this study, the attenuated

total reflectance (ATR) accessory was accessed, because only the surface studies of the materials were only needed. For the analysis, each sample of the sugarcane peel (Raw, CPC and CNC) was placed on the diamond crystal and the ATR holder was screwed onto the sample to have a direct contact with the crystal. The PerkinElmer spectrum 400 FTIR spectrometer was set to scan 60 times at a resolution of 2.0cm^{-1} over the wavelength range of 4000cm^{-1} to 650cm^{-1} against the transmittance. After each scan, the baseline was corrected using the background spectrum previously obtained from the blank

2.4.4 High resolution scanning electron microscopy (HRSEM)

HRSEM was used to observe the surface morphology of materials at a very minimal scale such as nanometer and micrometer. The samples were prepared by coating with carbon to make SEM analysis conductive, Emitech K950X carbon evaporator was used for the coating process.

The instrument produces a beam of electrons that hits the specimen ensuing in the emission of X-rays. The electron recorder takes up the rebounding electrons. The information from the electron recorder is converted onto a screen as three dimensional images. Apart from images HRSEM can also use energy dispersive X-ray spectroscopy (EDX) to determine the elemental composition and elemental mapping. In this study AURIGA Field Emission High Resolution Scanning Electron Microscope was used to analyse the surface morphology of the untreated, treated and the nanocrystal. The sample images from HRSEM were taken at different magnification.

2.4.5 Transmission Electron Microscopy (HR-TEM)

TEM is an instrument used to define the detailed morphology and nanocrystalline sizes of the CNCs. In the operation of TEM, the electron beams penetrate and interact with atoms of the materials, hereby leading to scattering of electrons. In this study TEM was used to study the internal structure and particle size of the CNC. The sample was prepared by drop-coating one drop of specimen solution onto a carbon coated copper grid. This was then dried under a xenon lamp for 10minutes, thereafter the sample coated grids were analysed under microscope. Transmission electron micrograph were collected using FEI Tecnai G2 F20 field emission gun (FEG) TEM, operated in bright field mode at an accelerating voltage of 200kV.

2.4.6 X-ray Diffraction (XRD)

X-ray diffraction (XRD) is a technique used to identify the crystallinity nature of a material, which could be minerals, organic or inorganic. However, in this study the analysis was carried out to check the crystallinity nature of the raw, CPC and CNC samples. Also, it's used the check the particle sizes of the untreated and treated samples-ray diffraction is based on the principle of bombarding material with accelerated electrons which invariably leads to the dislodgement of inner shell electron of the material, hence generating X-rays in relation to the rotating angle of the

sample and the detector. For this research X-ray was carried out using Philips X-pert MPD X-ray diffractometer with Cu-K radiation operated at 40 kV and 40 Ma. The sample was scanned over a range of 5 ° to 70 ° 2θ with the count step size set at 0.5 seconds per step/0.05 step size. The crystallinity index (CI) was calculated from the maximum intensity of the principle peak of 200 (I₀₀₂, 2θ= 22.71°) and the intensity of diffraction of 110 peaks (I_{am}, 2θ=15.02°) using the Segal method ((Azubuiké et al., 2012; Seagal et al., 1959).

I₀₀₂ represents both crystalline and amorphous material, whereas I_{am} represents the amorphous material.

$$CI (\%) = \left(1 - \frac{I_{am} \times 100}{I_{002}}\right)$$

2.4.7 Thermogravimetric Analysis (TGA)

Thermal gravimetric analysis or thermogravimetric analysis (TGA) is a technique used to determine changes in the physical and chemical properties of a materials by measuring the weight loss as a function of increasing temperature (with constant heating rate), or as a function of time (with constant temperature and/or constant mass loss). The loss in weight can be as a result of changes in the mass of a sample due to decomposition, oxidation or loss in moisture content. In overall, a mass less than 5.0g of sample was required and the result was plotted on the screen as the sample loss weight with an increase in temperature. Thermal stability of the raw, CPC and CNC were performed using PerkinElmer thermogravimetric analyser TGA 4000. About 3.0 mg Of each sample was weighed using a crucible sample holder and then placed in the machine. The TGA analysis was conducted under nitrogen atmosphere and the heating rate of the sample was set at room temperature, 25 °C/min up to 700 °C and then held for 1 minute at 700 °C.

2.4.8 Zeta Potential Measurement

Zeta potential is a technique used to measure or examine dispersion stability of colloids, indicating the degree of electric charge at the surface of the nanospheres. Zeta potential values were evaluated by determining the electrophoretic mobility using the Zetasizer Nano Series (Malvern Instruments, Malvern, UK). In this study, the measurement were performed in samples previously diluted in 0.005M NaCl. The samples were injected into DTS1060C/ DTS1070 zeta cell (Malvern) sample cells through a 0.45 µm PVDF filter to remove raw, CPC and CNC aggregates and larger impurities at a temperature of 25 °C for 180 s and were measured using PALS technology. The measurement was repeated three times for each sample and the average Zeta value was recorded alongside with the polydispersity index value.

2.5 Physicochemical Properties of Cellulose Nanocrystal.

2.5.1 Moisture Content

The samples (CP, CPCPC and CPCNC) of 0.5 g each was measured into a crucible. This was put in a drying oven and heat applied for 5 h at constant temperature of 105 °C until a steady mass was achieved. The change between the mass constituents was calculated as shown in Equation 2:

$$\% \text{ moisture content} = \frac{m_2 - m_3}{m_2 - m_1} \times 100 \dots \dots \dots \text{Equ. 2}$$

Where, m_1 = mass of the crucible with lid

m_2 = mass of crucible with lid and sample before drying

m_3 = mass of the crucible with lid and sample after drying

2.5.2 pH Determination of the Nanocrystal

pH of the sample was ascertained by measuring 1 g of each of the samples, which was heated in the beaker with a 100 cm³ capacity of distilled water for 5 minutes; the solution was watered down to 200 cm³ with distilled water and allowed to cool at a temperature of about 25 °C. The pH of each sample was ascertained using a Mettler Toledo, SCS 220K pH meter and the result was reported.

2.5.3 Determination of Loss of Mass on Ignition

This was carried out by weighing 0.05 g of the samples and put in furnace at constant temperature of 600 °C for 3 h. After heating, the sample was charred and removed from the furnace then placed in a desiccator to cool. The remaining product is then weighed, and the difference in mass denotes the mass of organic material present in the sample.

2.5.4 Swelling Capacity (SWC)

The swelling capacity was determined according to Hongjia et al. (2013); Adewuyi and Vargas 2017. 0.1 g (M) of samples was measured accurately and put into a calibrated tube and its first bed volume was recorded as V1, and mixed with 1 mL of distilled water and shaken well. The tubes having water and sample were then placed in water bath at 25 °C for 24 h, and the final bed volume of the sample was recorded as V2. The swelling capacity was calculated using Equ. 3

$$\text{SWC (ml/g)} = \frac{V2 - V1}{M} \dots \dots \dots \text{Equ. 3}$$

2.5.5 Water holding capacity (WHC)

The water holding capacity was measured using the method of Hongjia et al. (2013); Adewuyi and Vargas (2017), Zhang et al., (2005). A cleaned centrifuge tube (M) was weighed and measured. 0.1 g (M1) of sample was placed in 7 mL of distilled water and transferred into the centrifuge tube placed in a water bath at 37 °C. The tube was held for 30 min, followed by centrifugation for 15 min at 4000 rpm. The supernatant was decanted and the calibrated centrifuge tube with the wet sample (M2) was weighed again. The water holding capacity was calculated using Equ. 4

$$\text{WHC (g/g)} = \frac{M2 - (M + M1)}{M1} \dots \dots \dots \text{Equ. 4}$$

2.5.6 Oil holding capacity (OHC)

The oil holding capacity was measured by a method by Hongjia et al. (2013); Adewuyi and Vargas (2017), Abdul-Hamid and Luan (2000). 0.2 g (M) of sample was mixed with 1 mL olive oil (V1) in a 15 mL calibrated centrifuge tube. The solution in the centrifuge tube was stirred for 30 s in every 5 min, and 30 min after this the solution in the centrifuge tube was centrifuged at 3800 rpm for 25 min. The oil (V2) in the centrifuge tube was decanted and the absorbed oil was determined by the difference between V1 and V2. The oil holding capacity was calculated using Equ. 5

$$\text{OHC (ml/g)} = \frac{V2 - V1}{M} \dots \dots \dots \text{Eqn 5}$$

3.0 Results and Discussion

3.1 Chemical Composition

Chemical composition of cassava peel in table 1 shows that the cassava peel consist of 7.075±0.015% cellulose, 11.01±0.01% hemicellulose, 65.035±0.005% lignin and 16.85±0.02% wax. The value of cellulose obtained in this study was low compared to 93.24% reported by Widiato et al., 2017; Leite et al., 2017 reported cellulose yield of 14.8±0.8% which is relatively similar to that obtained in this study.

Table 1

Chemical composition analysis of lignocelluloses of cassava peel

Sample	Cellulose (%)	Hemicellulose (%)	Lignin (%)	Wax (%)
Cassava Peel	7.075±0.015	11.01±0.01	65.035±0.005	16.85±0.02

3.2 Yield of CNC

The percentage yield of CPCNC in this study was 6.42%, which is relatively similar to that reported by Widerto et al., 2017 and Leite et al., 2017; 17.80 and 10.5% respectively.

3.3 FTIR Analysis

The FT-IR technique was analysed to study the functional groups present in cassava peel (CP). Fig. 1 shows the FTIR spectra of cassava peel; CP, CPCPC and CPCNC, the characteristic strong band that appeared at 3333 cm⁻¹ and 3272cm⁻¹ for CNC, CPC and CP respectively, which is associated to the stretching vibration of O-H groups having strong inter- and intra-molecular H-bonding. CNC, CPC and CP showed a stretching frequency at 2892 cm⁻¹, 2906cm⁻¹ and 2920cm⁻¹ respectively was due to the symmetric C-H vibrations and 1640 cm⁻¹ and 1625cm⁻¹ emanated from the absorbed water. Peaks at 1412, 1319 and 1426 cm⁻¹ of CP, CPCPC and CPCNC are due to the bending of CH, CH₂ and OH respectively, which indicates polysaccharides and 1163 and 1149cm⁻¹ of CNC, CPC and CP are due to asymmetric vibrations (C=O=C) (Naduparambath, 2018; Nascimento et al., 2016) The characteristic peaks of cellulose were obvious at frequencies 1035 and 1007 cm⁻¹ of CNC, CPC and CP respectively corresponds to C=O=C stretching vibration of pyranose ring (Deepa et al., 2015; Ilyas et al., 2017). The peak at 765cm⁻¹ in the raw sample disappeared in the treated sample indicating the removal of silica.

The peaks between 1398 and 1177cm^{-1} of the nanocellulose is indicative of sulfonates in nanocellulose sample (Morais et al., 2013).

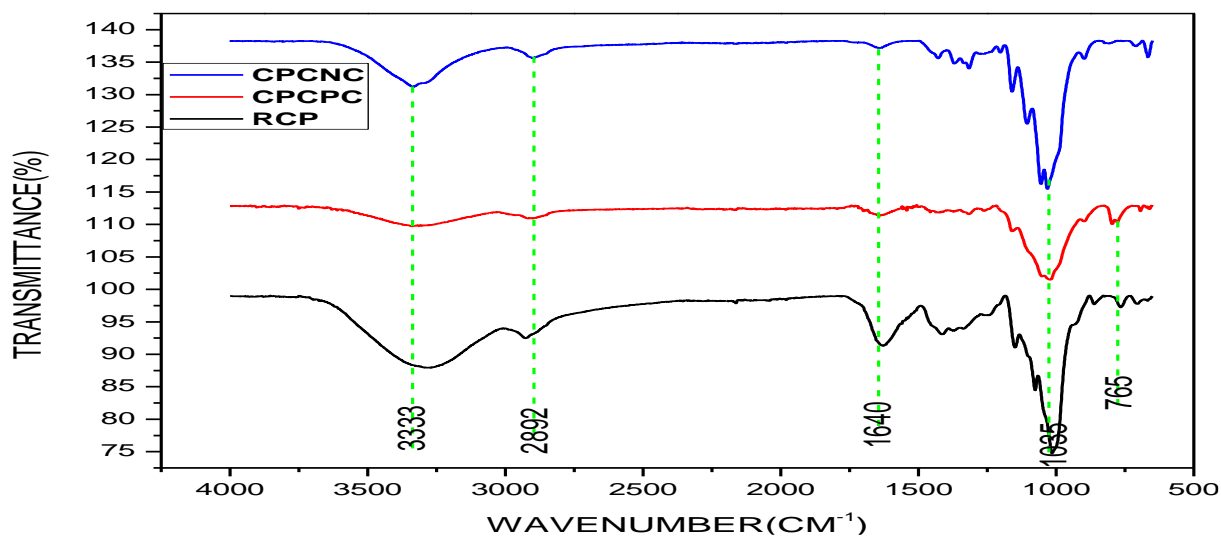


Fig. 1. FTIR spectra of raw cassava peel (RSP), cellulose fibre (SPCPC), cellulose nanocrystal (CPCNC)

3.4 SEM analysis

The SEM images are shown in Fig 2. The raw cassava peel has a diameter bigger than the CPC and CNC, comprising of different microfibrils which is similar to that reported by Arup and Debabrata, 2011. The smooth surface of the untreated sample of the cassava peel is due to the presence of some non-fibrous components in the fibre surface such as lignin, hemicellulose, wax, pectin, oil etc., On subsequent treatment with alkaline and bleaching with acidified sodium chlorite, it is evident that hemicellulose and lignin were removed as revealed by Ilyas et al., 2018; Arup and Debabrata, 2011.

The alkaline treatment reveals that the hemicellulose was hydrolyzed and becomes water soluble, the fibrils were defibrillated. After chemical treatment of the raw fibre, a narrow fibril and reticular structure of the fibre which is the chemically purified cellulose was seen, indicating that the procedure of purifying and bleaching did not completely break the cellulose structure and remove impurities while the cellulose nanocrystal fibre was broken completely into individualize nanocrystal, indicating complete removal of the amorphous domain. The surface morphology of the raw samples was different from that of the CPCS with a decrease in diameter which may have ensued from the removal of lignin, hemicellulose and other non-cellulosic constituents (Adewuyi and Vargas, 2016, Chen, et al., 2011). Moreso, the surface of CPCS also presented a lump like structure, which may be due to the strong intramolecular hydrogen bonds that occur in the molecule, also the smooth surface of the nanocrystals revealed that the addition of sulphuric acid into cellulose units of the CPCS may have narrowed the production of the intramolecular hydrogen bonds (Adewuyi and Vargas, 2016).

Features of the cellulose nanocrystal in the cassava peel, showed that there was a reduction in the fibrillar structure size and intermittent breakdown in fibrillar structure into individualize fibrils. Fig.2c represents the freeze dried cellulose nanocrystal, the structure of the cellulose was absolutely shattered and the size was considerably reduced to nanosize as pointed out by Hongija, et al., 2013.

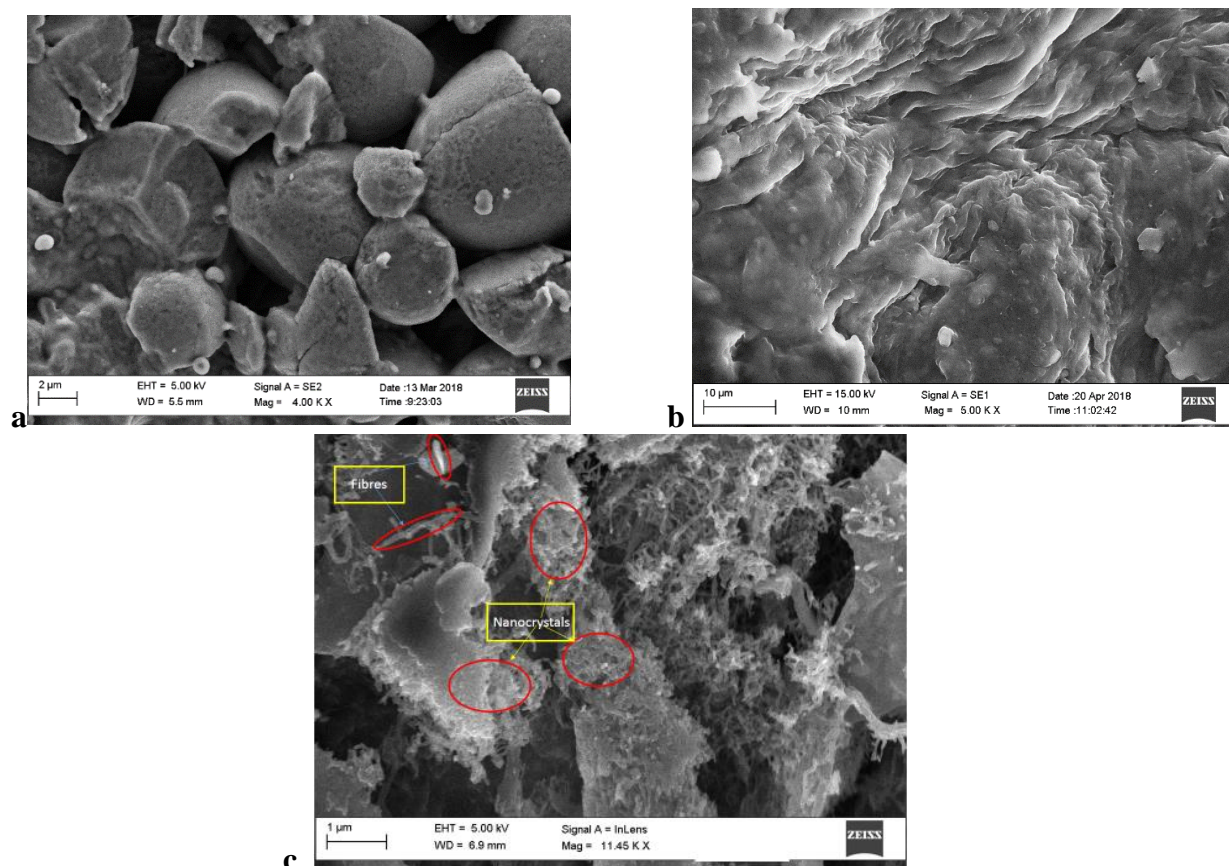


Fig.2 Scanning electron micrograph of (a) untreated cassava peel; (b) chemically purified cellulose i.e., cellulose; and (c) cellulose nanocrystal

3.5 Elemental Analysis of the Cellulose Nanocrystals

The elemental analysis of the cassava peel sample was carried out using EDX coupled with HRSEM. The EDX spectrum of the cellulose nanocrystal is shown in Fig.3. The results presented in Table 2 showed the presence of 0.70 wt. % elemental sulfur impurity with the major components of 73.89% for carbon and 25.41% for oxygen of cassava peel cellulose nanocrystal. The quantity of sulfur present might have emanated from the sulfate group during treatment with sulphuric acid hydrolysis.

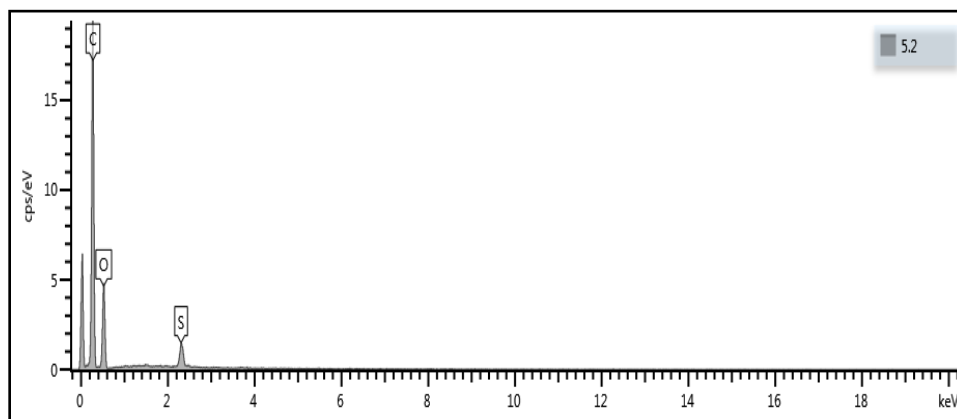


Fig. 3 Energy-dispersive spectroscopy spectrum of cellulose nanocrystal from cassava peel

Table 2

Chemical composition obtained from EDX of Cellulose nanocrystal from cassava peel

Element	Atomic %
C	73.89
O	25.41
S	0.70
Total:	100.00

3.6 TEM analysis

The TEM image in Fig. 4 shows that the cassava peel sample is spherical in shape, conglutinated and fixed with each other. This is an indication that the CNC is very small and specific area is large. The sizes of nanocellulose dependent intensely on the protocol and hydrolysis conditions (Naduparambath, et al., 2018). In overall, strong acid concentration, longer reaction time and higher temperature might yield short CNCs (Naduparambath, et al., 2018, Martínez-Sanz, et al., 2011). The CPCPC and CPCNC were characterized and analyzed by particle length (L), width (W). The diameters and length of the fibers after hydrolysis treatments were calculated by an image processing analysis program, Image J, using TEM images. Fig. 4(a) and (b) revealed that, the CNC of cassava peel have spherical shaped particles with a width range of 9.75-49.02nm and an average width value of 25.78 ± 9.60 nm and length range of 19.51-107.76nm, with an average length value of 46.08 ± 20.28 nm which is similar to that reported by Hongjia, et al., 2013. Lu and Hsieh, 2010 reported that most samples from acid hydrolysis and freeze-drying were spherical cellulose nanocrystals. The sources of these cellulose spheres could be from self-assembled short cellulose rods through interfacial hydrogen bonds, the isolated spherical cellulose nanocrystals reported were in 10–100nm diameters, also spherical cellulose nanocrystals by acid hydrolysis have been reported by Zhang et al., 2007. The ultrasonic treatment might play an important role in forming the spherical CNC (Naduparambath, et al., 2018, Wang et al., 2007). It is possible that the network structured cellulose nanocrystals are embedded in the abundant spherical cellulose nanocrystals in the freeze drying process. Another reason is that the network structured cellulose was actually formed by the over-irradiation of electron beams during TEM analysis (Lu and Hsieh, 2010). The image of the CPCPC evidently revealed a less clear morphologies than the CPCNC, this indicates that the CPCPC has more amorphous region than the nanocrystal and the size dimension is larger compared to the nanocellulose (Wulandari et al., 2016). The histograms of TEM image of CNCs are shown in Fig. 4 c, d width and length respectively.

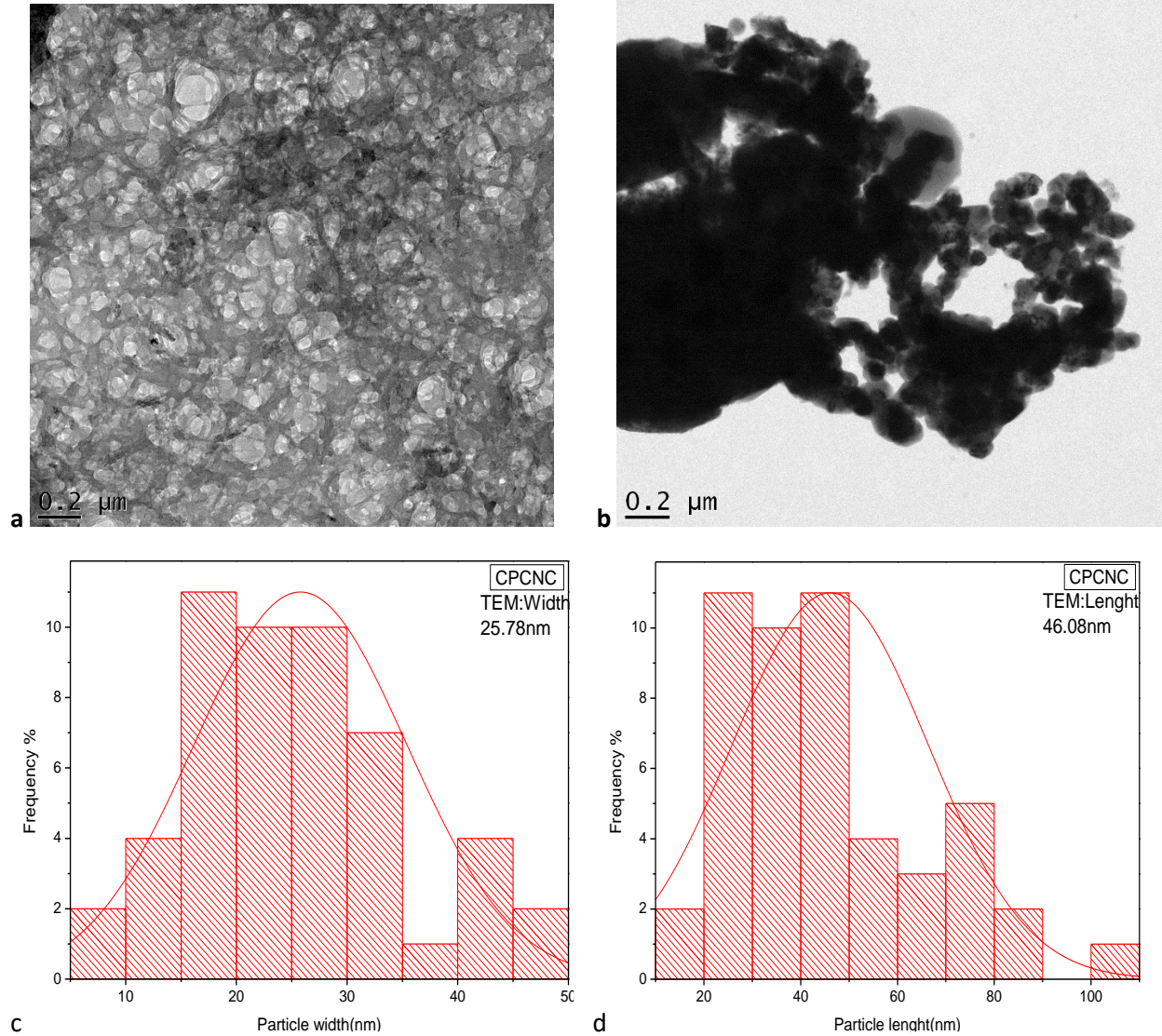


Fig. 4 TEM images of (a) cellulose nanocrystal (b) chemically purified cellulose (c) histogram of CNC (c) width (d) length

3.7 Zeta potential analysis

Zeta Potential analysis is an important instrument for understanding the state of the nanoparticle surface and envisaging the long term stability of the nanoparticle (Nanocomposix, 2012). Nanocellulose crystals with a zeta potential value of less than -30 mV and greater than 30 mV have a high degree of stability (Mohaiyiddin et al., 2016). Fig.5 (a and b) shows the zeta potential of isolated cassava peel (CPCNC) and CPCPC respectively, this revealed the presence of negative charge on the surface of the CNC, formed by grafting of sulphate groups due to sulphuric acid hydrolysis which induces the formation of a negative electrostatic layer covering the nanocrystals and promotes their dispersion in water (Khouri, 2010, Naduparambath, et al., 2018). Nanocellulose crystals with stable suspension should have a zeta potential value of less than -30 mV and greater than 30 mV (Mohaiyiddin et al., 2016) or higher than 25 mV (Shaheen and Emam, 2018, Morais et al., 2013). Agglomeration of nanocellulose will arise if the zeta potential value is within the

range of -15 mV (Khouri, 2010, Naduparambath et al., 2018). Nanocellulose particles within this range don't have adequate charge to repulse each other, thereby forming agglomeration. The isolated CPCNC have a zeta potential value of $-20.7 \pm 8.12\text{ mV}$ respectively, which shows a negative zeta potential. Negative zeta potential below -30 mV indicates their ability to be stable in colloid ((Faradilla et al., 2016).

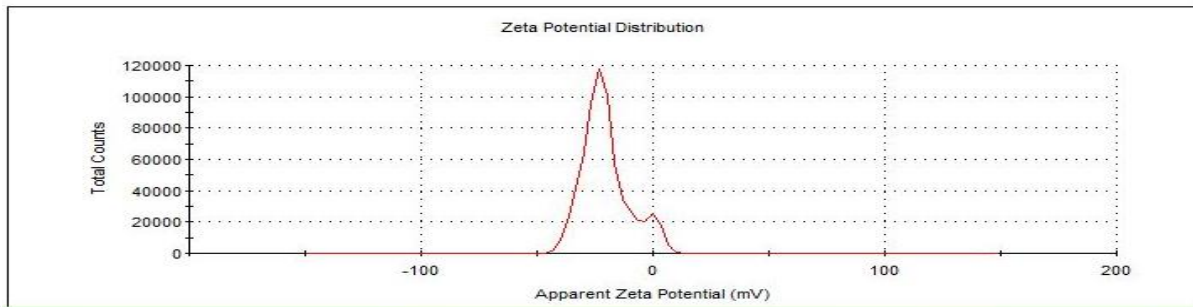
Zeta potential value for CPCNC shows a high zeta potential which indicates a partial agglomeration in solution due to Vander Waal inter particle attraction, the zeta potential indicates agglomeration of the particles. (Nanocomposix, 2012, Shaheen and Emam, 2018, Emam et al., 2017). If the result quality field indicates good, then there is a uniform zeta potential distribution between runs and a high quality phase plot (Nanocomposix, 2012). The presentation of the nanocellulose as an adsorbent and reinforcing agent is related with surface charge (zeta potential). Since the surface charge is negative, these indicates a good surface for adsorption and several other applications.

The zeta potential of the chemically purified cellulose of the cassava peel, showed a change from the nanocellulose with values of $-1.78 \pm 2.96\text{ mV}$, leading to agglomeration of the CPCPC (Moraian et al., 2016, Shaheen and Emam, 2018), Thus, the disperse stability of nanocellulose could be due to the presence of sulfate group (SO_4^{-2}) arising from hydrolysis of cellulose with sulfuric acid. Due to the negative charges on the surface of the CNCs, the electrostatic repulsion force between the two electrical layers inhibits CNC from agglomeration in solution.

More so, the Poly-Dispersity Index (PDI), represents basically the molecular weight distribution throughout the polymer. The PDI values of CPCNC and CPCPC are 0.633 and 0.842 respectively. PDI values greater than 0.7 indicates that the sample has a broad size distribution. A high value shows a polydisperse system and low value shows a monodisperse system. Polydisperse have a greater tendency to aggregate than a monodisperse system. Also, if PDI is greater than 1, it indicates that the polymer has extra chains as compare to actual molecular chain. It may be transesterification (like cyclic oligomers) or chain transfer products.

	Mean (mV)	Area (%)	St Dev (mV)
Zeta Potential (mV): -20.7	Peak 1: -22.3	96.3	8.12
Zeta Deviation (mV): 9.14	Peak 2: 4.19	3.7	1.61
Conductivity (mS/cm): 0.674	Peak 3: 0.00	0.0	0.00

Result quality : Good



a

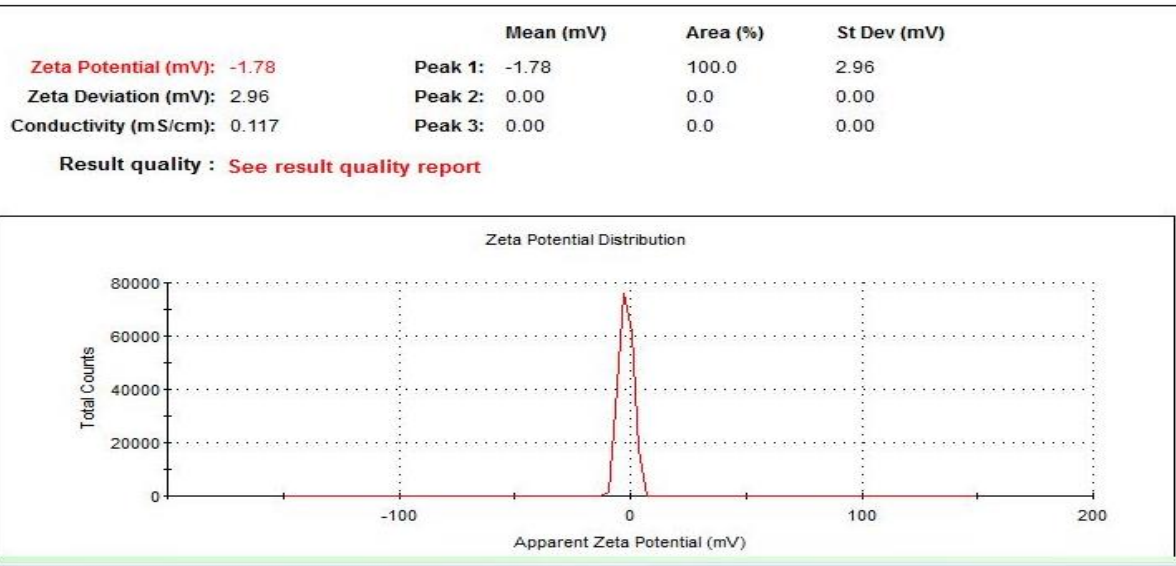


Fig.5 Zeta potential measured from zetasizer analyzer for CPCNC and CPCPC of cassava peel

3.8 X-RAY DIFFRACTION

The crystalline structure and phase purity of cassava peel (CP, CPCPC and CPCNC) were analyzed by X-ray diffraction analysis. XRD pattern of cassava peel, cassava derived CPCs and isolated CNCs are shown in Fig. 6. The characteristics peaks for the raw sample absorbed at $2\theta = 17.65^\circ$, 15.02° and 34.19° which corresponds to 110 and 004 lattice planes of cellulose I respectively, indicating the presence of lignin and hemicellulose (Ilyas et al., 2016, Lu and. Hsieh, 2010). Also, the peaks at $2\theta = 12.39^\circ$ and 22.71° for CPC, which correspond to lattice planes of 110 and 200, indicating cellulose II and the disappearance of the peak at 004 indicates the partial removal of amorphous region (Thambiraj and Shankaran, 2017, Klemm et al., 2005). The low intense peak at $2\theta = 12.0^\circ$ of the CNC indicates the complete removal of the amorphous region. The broad peak of the CNC indicates the removal of the amorphous region which results in increasing the degree of crystallinity, resulting into broader surface area and higher tensile strength of the CNC. The major intensity peak that was identified in the X-ray diffractograms which is located at 2θ value of around 22.71° shows the crystallinity structure of cellulose I for all samples, whereas the low intensity peak at a 2θ value of around $12^\circ - 14^\circ$ was labelled as amorphous region (Rahimi et al., 2016). The crystallinity index of CP, CPCPC and CPCNC was calculated to be 60.70%, 91.72%, and 99.86%, respectively which is similar to the result obtained by Mohamad et al., 2017. The crystallinity index increased progressively from the raw to the CNC which is similar to the trend of results obtained by Nurian et al., 2012, Rahimi et al., 2016. The progressive increase from raw to CNC implies the removal of lignin, hemicellulose and extractive according to Buong et al., 2017, Widiarto et al., 2016 and Zain et al., 2014. The XRD crystallite particle size for cassava peel showed a trend from untreated to CNC to be 25.39, 24.10 and 5.56 nm respectively, and these results corresponds to that obtained from TEM.

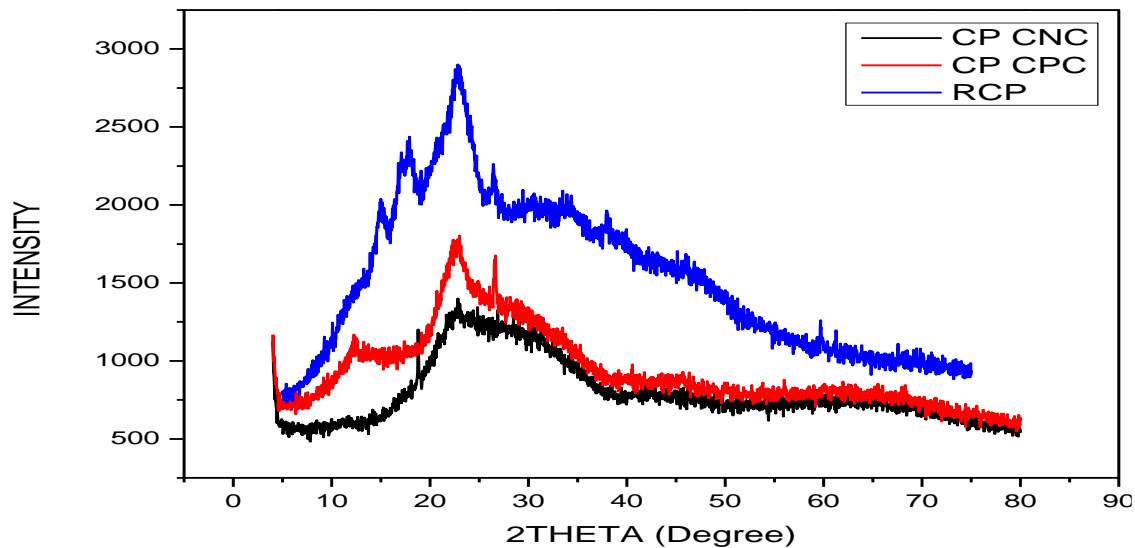


Fig. 6 X-ray diffraction patterns of raw cassava peel (RCP), cellulose (CPCPC), cellulose nanocrystal (CPCNC)

3.9 Thermogravimetric analysis (TGA)

Studying the thermal properties of natural fibres is a key factor in order to determine their heat stability for compatibility in various applications. (Ilyas et al., 2016).

Fig. 7 a and b shows the TGA and DTG graph of the untreated, treated and nanocrystal of cassava peel. The raw cassava peel, have three inflation point, at temperature of maximum degradation which occurred at 75.26 °C due to evaporation of moisture in the raw cassava peel (CP). The next weight loss was due to hemicellulose decomposition that occurred at 245.56 °C for the untreated fiber, and this loss can be associated to the depolymerization of hemicellulose (Yang et al., 2007). The CPCPC and CPCNC showed two inflation points. Hence, the disappearance of peaks due to sample treatments indicates that the amorphous domains were removed because of the breakdown of ether and carbon-carbon linkages (Joseph, 1999). The peak in the range of 300–400 °C, that reaches the maximum rate of decomposition, is attributed to the glycosidic cleavage of cellulose. The CPCPC showed a weight loss at 100.54 °C due to moisture evaporation and a maximum degradation temperature at 349.51 °C. From the TGA graph, it showed that the CNC is less thermally stable because it degraded faster than the CPC and raw and it degraded uniformly unlike the raw, which has different endothermic peaks.

The nanocrystal showed an initial weight loss at 70.20 °C, which was due to evaporation of water and temperature of maximum degradation at 292.33 °C and a Temperature onset (thermal stability of the sample) at 218.22 °C. The raw sample of cassava peel fiber showed an endothermic peak at 317.42 °C. The CPC showed peaks at 349.51 °C with Temperature onset at 248.56 °C (Leoa et al., 2016, Lavoratti et al., 2016). The endothermic peak of cellulose nanocrystals was reduced compared with the CPCPC and CP sample, this is due to the attachment of sulfate groups in the cellulose nanocrystals' surface during the hydrolysis with sulfuric acid (Leoa et al., 2016, El Miri et al., 2015). This statistic is also reported in cellulose nanocrystals isolated from Curaua (Corradini et al., 2016) with a temperature onset of 209 °C. The raw sample and the CPC was similar with that reported by Hongjia et al., 2013) on cellulose nanocrystals obtained from sweet potato (raw at 327 °C and treated 336 °C).

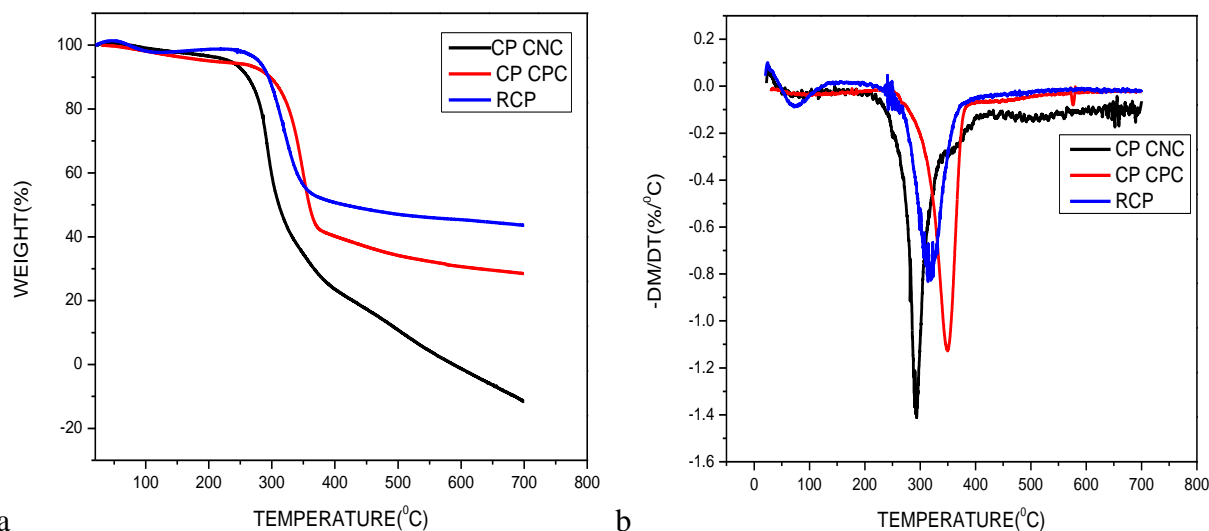


Fig. 7 (a) TG and (b) DTG curves for raw cassava peel, cellulose and nanocrystal of cassava peel

3.10 Physicochemical Properties of Untreated, Treated and Cellulose Nanocrystals of Cassava Peel

3.10.1 pH

pH is a measure of hydrogen ion concentration of a solution. The value reported in this study showed that the pH of cassava peel is acidic 4.59 as compared to CPCPC and CPCNC which are neutral, 6.61 and 6.38 respectively this is expected since they were washed and dried at neutral pH.

3.10.2 Moisture Content

The determination of moisture content is an important characteristic as potential adsorbent, bio-composite, food packaging and various industrial applications. It is used to evaluate the properties and the final uses of fibre materials. High moisture content of fibres could deteriorate the stability of cellulose materials in terms of tensile strength, formation of porosity and size (Ilyas et al., 2018; Jumaidin et al., 2017a, 2017b, 2017c). In this study the moisture content of RCP, CPCPC and CPCNC are 18.01 ± 0.01 , 8.745 ± 0.005 and $7.295 \pm 0.005\%$ respectively. The raw samples have higher moisture content when compared to the treated sample and the nanocrystals of the sugarcane peel, this could be due to the presence of hydroxyl functional groups in the parent materials than the CPCs and CNCs, so the higher hydroxyl group content may have aided the interaction with water molecules and as such giving it a higher hydration property (Adewuyi and Vargas, 2017).

3.10.3 Loss of Mass on Ignition

These test methods cover the determination of the mass loss from solid combustion residues upon heating in an air to a prescribed temperature. (ASTM D7348, 2018)

Loss of mass on ignition for cassava peel decreased from raw to the nanocellulose, the values obtained are as follows; RCP, CPCPC and CPCNC 4.91 ± 0.00 , 4.765 ± 0.005 and $4.59 \pm 0.02\%$ respectively, this could be due to the presence of hydroxyl functional groups in the raw material, the high hydroxyl content may have aided the interaction with water molecules as such having more water property (Adewuyi and Vargas, 2017). This result also confirms the high moisture

content in the cassava peel. The values gotten, revealed a decrease from raw to nanocellulose in this order; CP, CPCPC and CPCNC (18.01 ± 0.01 , 8.745 ± 0.005 and 7.295 ± 0.005).

3.10.4 Swelling Capacity

This is the amount of liquid that can be absorbed by a cellulosic fibre. The raw sample of the cassava peel has a higher swelling capacity when compared to the treated samples. The result is as follows; RCP, CPCPC and CPCNC, 2.5 ± 0 , 1.55 ± 0.05 and 1.0 ± 0.05 mL/g respectively. This tallies with the result revealed by (Adewuyi and Vargas, 2017), it indicates the ability of the raw to hold water molecules. This could also be due to the presence of hydroxyl functional groups in the parent material than the CPC and CNC, so the higher hydroxyl group content may have aided the interaction with water molecules and as such giving it a higher hydration property (Adewuyi and Vargas, 2017).

3.10.5 Water Holding Capacity

Water holding capacity is the ability of a material to hold water alongside with its own water when undergoing processing. (Adewuyi and Vargas, 2017). Water holding capacity of a material is reliant on several reasons such as inherent chemical and physical structure (Grigelmo-Miguel and Martin-Belloso, 1999). The obtained result is as follows, RCP, CPCPC and CPCNC; 3.528 ± 0 , 3.8675 ± 0.0005 and 5.0225 ± 0.0005 g/g respectively. The trend of the result is similar to Hongjia, et al., (2013). The treated cellulose nanocrystals exposed more surface area, uronic acid group and water binding sites to the surrounding (Hong and Zhang, 2005 and Lu et al., 2013). The higher water holding capacity of the nanocrystals over the raw and the chemically purified cellulose suggests the possible use of CPCNC in water treatment (adsorbents), paper and pulp, pigments and in food applications where low moisture retention is required (Adewuyi and Vargas, 2017 and Hongjia et al., 2013). More so, good water holding capacity is important for stability and texture, it is necessary to consider microbial activity and safety of a material which may affect shelf life.

3.10.6 Oil holding Capacity

Oil holding capacity is associated with adsorption of organic compounds to the surface of the substrates (Adewuyi and Vargas, 2017; Biswas et al., 2009). The oil holding capacity of the CNC of cassava peel is higher than the raw sample. It indicates that the reduction of cellulose size and bulk density with the introduction of sulphate group during acid hydrolysis might have increased the porosity and superficial area of the fiber, improve and promote the physical entrapment of oil and the magnitude of oil holding capacity (Adewuyi and Vargas, 2017, Lu et al., 2013 and Chau et al., 2007). The trend of the result is as follows; RCP, CPCPC and CPCNC; 4.95 ± 0.05 , 6.45 ± 0.05 and 7.05 ± 0.05 mL/g respectively.

Thus, the SEM image result further confirms the assertion due to the compact structure of the raw samples. The high OHC of the cellulose nanocrystal indicated that it has potential in food industry (Lu et al., 2013).

Table 3

Physicochemical properties of raw, chemically purified cellulose and cellulose nanocrystals from cassava peel

Sample	Swelling Capacity (mg/g)	Water Holding Capacity (g/g)	Oil Holding	Loss of Mass on Ignition (%)	Moisture Content (%)	pH

			Capacity(mg/g)			
RCP	2.5±0	3.528±0	4.95±0.05	4.91±0.00	18.01±0.01	4.59
CPCPC	1.55±0.05	3.8675±0.0005	6.45±0.05	4.765±0.005	8.745±0.005	6.61
CPCNC	1.0±0.05	5.0225±0.0005	7.05±0.05	4.59±0.02	7.295±0.005	6.38

4.0 Conclusion

The present study shows that cassava peel is an interesting source of raw material for the production of cellulose nanocrystal, due to the result of the various characterizations obtained. Isolation of cellulose from cassava peel was prepared by using two pretreatments methods; alkaline treatment and bleaching with acidified sodium chlorite. Acid hydrolysis was performed at 45°C for 45 mins using 64% concentration sulphuric acid. The Chemical composition consist of 7.075±0.015% cellulose, 11.01±0.01% hemicellulose, 65.035±0.005% lignin and 16.85±0.02% wax, the percentage yield was 6.42%. From the SEM image features of the cellulose nanocrystal in the cassava peel, showed that there was a reduction in the fibrillar structure size and intermittent breakdown in fibrillar structure into individualize fibrils; the TEM image showed that the cassava peel sample is spherical in shape, conglutinated and fixed with each other, with particle size value of 25.78±9.60 nm in width and length value of 46.08±20.28nm. The FTIR spectra of the CNC was identified as cellulose structures that showed effective removal of amorphous materials. XRD showed that the crystallinity index increased progressively from the raw to the CNC with CNC crystallinity index of 99.86% and a particle size of 5.56 nm The TGA curve revealed a good thermal stability for CNC. The Zeta Potential revealed a negative surface charge of -20.7±8.12 mV and a polydispersity index of 0.633. The results showed effective extraction of CNC from cassava peel (a waste material from agricultural process). This material has potential for various industrial applications such as in medicine, adsorption of toxic metals, bio-nanocomposites, food packaging etc.

Acknowledgment

The authors sincerely appreciate the financial contributions of TETFUND (Nigeria), NRF/RISA (South Africa), NMR facility, University of the Western Cape, South Africa, Mr. Yunus Kippie of School of pharmacy, UWC and the support of the research laboratory of Environmental and Nano Science Group, University of the Western Cape, Cape Town, South Africa for offering laboratories and equipment for our research.

References

1. Abdul, H. P. S., Bhat, A. H., and Ireana, Y., A. F. (2012). Green composites from sustainable cellulose nanofibrils: A review. *Carbohydrate Polymers*, 87(2), 963–979
2. Abdul-Hamid, A., and Luan, Y. S. (2000). Functional properties of dietary fibre prepared from defatted rice bran. *Food Chemistry*, 68, 15–19.
3. Abe, K., and Yano, H. (2009). Comparison of the characteristics of cellulose microfibril aggregates of wood, rice straw, and potato tuber. *Cellulose*, 16: 1017-1023.

4. Adewuyi, A. and Vargas, P. F. (2016). Chemical Modification of Cellulose Isolated from Underutilized Hibiscus sabdariffa via Surface Grafting: A Potential Bio-based Resource for Industrial Application. *Kem.Ind.*, 66(7-8):327-338
5. Alemdar, A., and Sain, M. (2008). Isolation and characterization of nanofibers from agricultural residues – Wheat straw and soy hulls. *Bioresource Technology*, 99(6), 1664–1671. <http://dx.doi.org/10.1016/j.biortech.2007.04.029>.
6. Anuj, K., Yuvraj, S. N., Veena, C. and Nishi, K. B. (2014). Characterization of cellulose nanocrystals produced by acid-hydrolysis from sugarcane bagasse as agro-waste. *Journal of Materials Physics and Chemistry*, 2(1): 1-8.
7. Arup, M. and Debabrata, C. (2011). Isolation of nanocellulose from waste sugarcane bagasse (SCB) and its characterization. *Carbohydrate Polymers* 86 (2011) 1291– 1299
8. ASTM D7348. (2018). Standard Test Methods for Loss on Ignition (LOI) of Solid Combustion Residues. <https://www.astm.org/Standards/D7348.htm>. DOI: 10.1520/D7348
9. Ayeni, A. O, Adeeyo, O.A., Oresegun, O. M., Oladimeji, T. E. (2015). Compositional analysis of lignocellulosic materials: Evaluation of an economically viable method suitable for woody and non-woody biomass *American Journal of Engineering Research (AJER)*, 4(4):14-19. e-ISSN: 2320-0847 p-ISSN: 2320-0936
10. Azubuike, C. P., Rodríguez, H., Okhamafe, A. O., & Rogers, R. D. (2012). Physicochemical properties of maize cob cellulose powders reconstituted from ionic liquid solution. *Cellulose*, 19(2), 425–433.
11. Beck-Candanedo, S., Roman, M., & Gray, D. G. (2005). Effect of reaction conditions on the properties and behavior of wood cellulose nanocrystal suspensions. *Biomacromolecules*, 6(2), 1048–1054.
12. Biswas, A.K., Kumar, V., Bhosle, S., Sahoo, J., Chatli, K. (2009). Dietary fibre as functional ingredients in meat products and their role in human health, *International Journal. Of Livestock. Production*. 2 (4) (2009) 45–54.
13. Buong, W. C., Syn, H. L. Nor, A. I., Yoon, Y. T. and Yuet, Y. L. (2017). Isolation and Characterization of Cellulose Nanocrystals from Oil Palm Mesocarp Fiber. *Polymers*, 2017(9):1-11. doi:10.3390
14. Chau, C. F., Wang, Y. T., & Wen, Y. L. (2007). Different micronization methods significantly improve the functionality of carrot insoluble fibre. *Food Chemistry*, 100, 1402–1408.
15. Chen, W. S., Yu, H. P., Liu, Y. X., Chen, P., Zhang, M. X., Hai, Y.F. (2011). Individualization of cellulose nanofibers from wood using high-intensity ultrasonication combined with chemical pretreatments, *Carbohydrate Polymer*. **83** (4):1804–1811, doi: (2016) 035004 doi:10.1088/2043-6262/7/3/035004
16. Chen, H. (2014). *Biotechnology of Lignocellulose: Theory and Practice*. Chemical Industry Press, Beijing and Springer Science CBusiness Media Dordrecht 2014 DOI 10.1007/978-94-007-6898-7__2

17. Corradini, E. A. G. P., Corrêa, A. C., E. M., Teixeira, E. M. and Mattoso, L.H.C.(2016).Thermal stability of cellulose nanocrystals from curaua fiber isolated by acid hydrolysis. *Cellulose Chemical Technology*, 50 (7-8), 737-743
18. Deepa, B., Abraham, E., Cordeiro, N., Mozetic, M., Mathew, A. P., and Oksman, K. (2015). Utilization of various lignocellulosic biomass for the production of nanocellulose: A comparative study. *Cellulose*, 22(2), 1075–1090.
19. Dufresne, A. (2012). Nanocellulose: From nature to high performance tailored materials. Walter de Gruyter.
20. El-Miri, N., Abdelouahdi, K., Zahouily, M., Fihri, A., Barakat, A., Solhy, A., (2015).Bio-nanocomposite films based on cellulose nanocrystals filled polyvinylalcohol/chitosan polymer blend. *Journal Applied Polymer Science*, 132, 1–13.
21. Elazzouzi-hafraoui, S., Nishiyama, Y., Putaux, J., Heux, L., Dubreuil, F., & Rochas, C. (2008). The shape and size distribution of crystalline nanoparticles prepared by acid hydrolysis of native cellulose. *Biomacromolecules*, 9(1), 57–65.
22. Emam, H. E., El-Zawahry, M. M. Ahmed, H. B. (2017). One-pot fabrication of AgNPs, AuNPs and Ag-Au nano-alloy using cellulosic solid support for catalyticreduction application, *Carbohydrate Polymer*. 166 (2017) 1–13.
23. Faradilla, R. H. F., Lee, G., Rawal, A., Hutomo, T., Stenzel, M. H. and Arcot, J. (2016). Nanocellulose characteristics from the inner and outer layer of banana pseudo-stem prepared by TEMPO-mediated oxidation. *Cellulose*, 23(5), 3023–3037.
24. Grigelmo-Miguel, N., and Martin-Belloso, O. (1999). Comparison of dietary fibre from byproducts of processing fruits and greens and from cereals, *LWT. Food Science Technology*, 32 (1999): 503– 508, doi: <https://doi.org/10.1006/fstl.1999.0587>.
25. Hong, J., and Zhang, S. Y. (2005). Effect of ultra-fine pulverization by wet processing on particle structure and physical properties of soybean dietary fiber in Chinese. *Journal of China Agricultural University*, 10: 90–94.
26. Hongjia, L., Yu G., Longhui, Z., and Xiong L. (2013). Morphological, crystalline, thermal and physicochemical properties of cellulose nanocrystals obtained from sweet potato residue. *Journal of Food Research International*, 50 (2013):121–128
27. Ilyas, R. A., Sapuan S. M., Lamin S. M., and Ridzwan I. M. (2017). Nanocrystalline cellulose as reinforcement for polymeric matrix nanocomposites and its potential applications: A review. *Current Analytical Chemistry*, 13. <http://dx.doi.org/10.2174/157341101366617100315562>
28. Ilyas, R. A., Sapuan, S. M., Ishak,M. R.(2018). Isolation and characterization of nanocrystalline cellulose from sugar palm fibres (*Arenga Pinnata*).
 - a. *Carbohydrate Polymers*, 181 (2018): 1038–1051.
29. Joseph, K., Filho, R. D. T., James, B., Thomas, S., and Carvalho, L. H. (1999). A review onsisal fiber reinforced polymer composites. *Revista Brasileira de EngenhariaAgricola e Ambiental*, 3, 379.

30. Julie Chandra C.S., Neena G, Sunil, K. N. (2016) Isolation and characterization of cellulose nanofibrils from arecanut husk fibre. *Carbohydrate Polymers* 142 (2016) 158–166
31. Jumaidin, R., Sapuan, S. M., Jawaid, M., Ishak, M. R., and Sahari, J. (2017a). Effect of seaweed on mechanical, thermal, and biodegradation properties of thermoplastic sugar palm starch/agar composites. *International Journal of Biological Macromolecules*, 99, 265–273. <http://dx.doi.org/10.1016/j.ijbiomac.2017.02.092>.
32. Jumaidin, R., Sapuan, S. M., Jawaid, M., Ishak, M. R., and Sahari, J. (2017b). Thermal, mechanical, and physical properties of seaweed/sugar palm fibre reinforced thermoplastic sugar palm starch/agar hybrid composites. *International Journal of Biological Macromolecules*, 97, 606–615. <http://dx.doi.org/10.1016/j.ijbiomac.2017.01.079>.
33. Jumaidin, R., Sapuan, S. M., Jawaid, M., Ishak, M. R., & Sahari, J. (2017c). Characteristics of *Eucheuma cottonii* waste from East Malaysia: Physical, thermal, and chemical composition. *European Journal of Phycology*, 0(0), 1–8. <http://dx.doi.org/10.1080/09670262.2016.1248498>.
34. Khouri, S. (2010). Experimental characterization and theoretical calculations of responsive polymeric systems. Waterloo, Canada: University of Waterloo M.Sc. dissertation.
35. Klemm D., Heublein B, Fink, H. P., and Bohn, A. (2005). Cellulose: fascinating biopolymer and sustainable raw material. *Angew Chem Int Ed*. 2005; 44:3358–3393.
36. Lavoratti, A., Scienza, L. C., and Zattera, A. J. (2016). Dynamic-mechanical and thermomechanical properties of cellulose nanofiber/polyester resin composites. *Carbohydrates Polymers*, 136, 955–963.
37. Leite, A. L. M. P, Zanon, C. D. and Menegalli, F. C. (2017). Isolation and characterization of cellulose nanofibers from cassava root bagasse and peelings. *Carbohydrate Polymers* 157 (2017) 962–970
38. Leão, R. M., Patrícia C. M., João M.L.L. M. and Sandra M. L. (2017). Environmental and technical feasibility of cellulose nanocrystal manufacturing from sugarcane bagasse. *Carbohydrate Polymers* 175 (2017): 518–529
39. Li, Q., Zhou, J., Zhang, L. (2009a). Structure and properties of the nanocomposite films of chitosan reinforced with cellulose whiskers. *Journal of Polymer Science, Polymer, Physical*. 47, 1069–1077.
40. Lu, P. and Hsieh, Y. (2012). Preparation and characterization of cellulose nanocrystals from rice straw. *Carbohydrate Polymers* 87 (2012) 564–573
41. Lu, P. and Hsieh, Y. (2010). Preparation and properties of cellulose nanocrystals: Rods, spheres, and network. *Carbohydrate Polymers*, 82(2): 329–336.
42. Lu, P., and Hsieh, Y. (2010). Preparation and properties of cellulose nanocrystals: Rods, spheres, and network. *Carbohydrate Polymers* 82 (2010) 329–336
43. Lu, H., Gui, Y., Zheng, L. and Liu, X. (2013). Morphological, crystalline, thermal and physicochemical properties of cellulose nanocrystals obtained from sweet potato residue. *Food Res. Int*. 50, 121–128.
44. Martínez-Sanz, M., Lopez-Rubio, A., and Lagaron, J. M. (2011). Optimization of the nanofabrication by acid hydrolysis of bacterial cellulose nanowhiskers. *Carbohydrate Polymers*, 85(1): 228–236.
45. Mohaiyiddin, M. S., Lin, O. H., Owi, W. T., Chan, C. H., Chia, C. H., Zakaria, S. (2016). Characterization of nanocellulose recovery from *Elaeis guineensis* frond for sustainable development. *Clean Technologies and Environmental Policy*, 18(8)

46. Mohamad, A. M., Salleh, W.N. W., Juhana, J. A.F., Ismailb, M. A. M., Abu, B. M., Zaind, M.F. M, Nor, A. A., and Zul, A. M. H.(2017).Physicochemical characterization of cellulose nanocrystal andnanoporous self-assembled CNC membrane derived from Ceiba pentandra. *Carbohydrate Polymers* 157 (2017) 1892–1902.
47. Moraisa, J.P. S., Rosab, M. F., Filhob,M. M. S., Nascimentoa, L.D., Nascimentob, D.M., Cassales, A. R. (2013). Extraction and characterization of nanocellulose structures from raw cotton linter. *Carbohydrate Polymers* 91 (2013) 229– 235.
48. Moriana, R., Vilaplana, F., and Ek,M.(2016), Cellulose nanocrystals from forest residues as reinforcing agents for composites: a study from macro- to nano-dimensions. *Carbohydrate Polymer*, 139 (2016): 139–149
49. Naduparambath, S., Jinitha, T.V., Shaniba, V., Sreejith, M.P., Aparna, K.B, and Purushothaman, E. (2018). Isolation and characterisation of cellulose nanocrystals from sago seed shells. *Carbohydrate Polymers*, 180 (2018): 13–20
50. Nanocomposix.(2012). Zeta potential analysis of nanoparticles. <https://www.scribd.com/document/355246162/nanoComposix-Guidelines-for-Zeta-Potential-Analysis-of-Nanoparticles-pdf.1-6>
51. Nascimento, D. M. D., Almeida, J. S., Vale, M. D. S., Leitão, R. C., Muniz, C. R., Figueirêdo, M. C. B. D. (2016). A comprehensive approach for obtaining cellulose nanocrystal from coconut fiber. Part I: Proposition of technological pathways. *Industrial Crops and Products*, 93, 66–75
52. Nurain, J., Ishak A., Alain D. (2012) Extraction, preparation and characterization of cellulose fibres and nanocrystals from rice husk. *Industrial Crops and Products* 37 (2012) 93– 99
53. Pelissari, F. M., Sobral, P. J. A. and Florencia C. M. F. C.(2014). Isolation and characterization of cellulose nanofibers from banana peels *Cellulose* (2014) 21:417–432 DOI 10.1007/s10570-013-0138-6
54. Pelissari, F.M., Sobral, P.J. A and Menegalli, F. C. (2014). Isolation and characterization of cellulose nanofibers from banana peels. *Cellulose* (2014) 21: 417–432 DOI 10.1007/s10570-013 0138-6
55. Rahimi, M. K. S., Brown, R. J., Tsuzuki, T. and Rainey, T. J (2016). A comparison of cellulose nanocrystals and cellulose nanofibres extracted from bagasse using acid and ball milling methods. *Advances in Natural Sciences: Nanoscience and Nanotechnology*, 7 (2016):1-9. doi:10.1088/2043-6262/7/3/035004
56. Rumpoko, W., Khaswar, S. Indah, Y. and Muhamad, N. (2013). Cellulose nanofibers from cassava bagasse: characterization and application on Tapioca-film. *Journal of Chemistry and Material Research*, 3(13): 79-87.
57. Seagal, L., Creely, J. J., Martin, A. E., & Conrad, C. M. (1959). An empirical method for estimating the degree of crystallinity of native cellulose using X-ray diffractometer. *Textile Research Journal*, 29, 786–794.
58. Shaheen,T. I. and Emam,H. E. (2018). Sono-chemical synthesis of cellulose nanocrystals from woodsawdust using Acid hydrolysis. *International Journal of Biological Macromolecules* 107 (2018) 1599–1606

59. Thambiraj S., and Ravi S. D. (2017). Preparation and physicochemical characterization of cellulose nanocrystals from industrial waste cotton. *Journal of Applied Surface Science* 412 (2017) 405–416
60. Wang, N., Ding, E., and Cheng, R. (2007). Thermal degradation behaviors of spherical cellulose nanocrystals with sulfate groups. *Polymer*, 48(12): 3486–3493.
61. Widiarto, S., Yuwono, S. D., Rochliadi, A. and Arcana, I. M. (2017). Preparation and Characterization of Cellulose and Nanocellulose from Agro-industrial Waste - Cassava Peel. *IOP Conference Series Material Science and Engineering*, 176 (2017) 012052 doi:10.1088/1757-899X/176/1/012052
62. Wulandari, W T, Rochliadi, A and Arcana I M (2016). *IOP Conference Series Material. Science. Engineering*. 107 012045
63. Yang, H., Yan, R., Chen, H., Lee, D. H., and Zheng, C. (2007). Characteristics of hemicellulose, cellulose and lignin pyrolysis. *Fuel*, 86(12–13), 1781–1788. <http://dx.doi.org/10.1016/j.fuel.2006.12.013>
64. Yang, S. H. (2008). *Plant fiber chemistry*. Beijing: China Light Industry Press; 2008.
65. Zain, N. F. M., Salma, M. Y., and Ishak, A. (2014). Preparation and Characterization of Cellulose and Nanocellulose from Pomelo (*Citrus grandis*) Albedo. *Journal of Nutrition and Food Science*, 5(1): 334. doi:10.4172/2155-9600.1000334
66. Zhang, J. G., Elder, T. J., Pu, Y. Q. and Ragauskas, A. J. (2007). Facile synthesis of spherical cellulose nanoparticles. *Carbohydrate Polymers*, 69(3), 607–611.
67. Zhang, M., Zhang, C. J., & Shrestha, S. (2005). Study on the preparation technology of superfine ground powder of *Agrocybe chaxingu* Huang. *Journal of Food Engineering*, 67, 333–337.

This study was carried out to investigate the potential use of cassava peel as a source of nanocrystalline cellulose. Isolation of cellulose from cassava peel was prepared by alkaline treatment and bleaching with acidified sodium chlorite. Acid hydrolysis was performed at 45°C for 45 mins using 64% sulphuric acid. The cellulose nanocrystal (CNC) from the cassava peel was characterised using, scanning electron microscope (SEM), x-ray diffraction (XRD), transmission electron microscopy (TEM), fourier transformed infrared spectroscopy (FTIR), thermogravimetric analysis (TGA) and zeta potential analysis. Physicochemical properties of the samples were studied. The FTIR spectra of the CNC was identified as cellulose structures that showed effective removal of amorphous materials. XRD showed a crystalline structure with CNC crystallinity index of 99.86 %. The TGA curve revealed a good thermal stability for CNC. The Zeta Potential revealed a negative surface charge of -20.7 ± 8.12 mV. The results showed effective extraction of CNC from cassava peel. This material has potential for various industrial applications.